Available online at www.sciencedirect.com
ScienceDirect
Journal of the European Ceramic Society 29 (2009) 2267–2273
www.elsevier.com/locate/jeurceramsoc

Study on structural evolution of nanostructured 3 mol% yttria stabilized zirconia coatings during low temperature ageing

Bo Liang [a,*], Chuanxian Ding [b], Hanlin Liao [c], Christian Coddet [c]

[a] State Key Laboratory of Metastable Materials Science and Technology, Yanshan University, Qinhuangdao, Hebei 066004, PR China
[b] Shanghai Institute of Ceramics, Chinese Academic of Sciences, Shanghai 200050, PR China
[c] LERMPS, Université de Technologie de Belfort-Montbéliard, 90 010 Belfort, France

Received 15 October 2008; received in revised form 3 January 2009; accepted 8 January 2009
Available online 8 February 2009

Abstract

In the present work, the nanostructured 3 mol% yttria stabilized zirconia coatings were deposited by plasma spraying, and its structural evolution during the low temperature ageing in wet atmosphere was investigated by Raman spectroscopy. The results showed that the nanostructured 3 mol% yttria stabilized zirconia coatings had lower resistance to low temperature ageing, although the nanostructured coatings have a metastable tetragonal-prime (t') crystal structure. The degradation mechanism was explained in terms of the diffusion of oxygen vacancies and OH^- ion and the reactions between OH^- and Y'_{Zr} ion. The microstructure of as-sprayed coating, especially the microcracks, plays a very important role in the low temperature degradation. It can enhance and accelerate the low temperature degradation. It was also verified by wavelength dispersive spectrometer (WDS) analysis that an yttrium-rich surface was formed due to the reaction between OH^- and Y'_{Zr} ion, which resulted in the transformation of t' to monoclinic zirconia phase.

Keywords: ZrO_2; Low temperature degradation; Nanostructured coating; Raman spectroscopy

1. Introduction

Plasma sprayed yttria-doped zirconia coatings have been widely used for the thermal protection of gas turbine engines and marine diesels, and considerably improved the combustion efficiency of engines.[1–3] To improve the lifetime of plasma sprayed yttried-doped zirconia coatings, many studies have been conducted on high temperature ageing and it is believed that the lifetime of plasma sprayed zirconia coatings was closely related to the transformation of tetragonal to monoclinic phase during ageing.[4–8] In fact, when plasma sprayed zirconia coatings were used in engine interiors as thermal barrier coatings, a low temperature degradation may take place due to the presence of moisture which is unavoidable during the fuel combustion process.

Since Kobayashi et al.[9] first reported the low temperature degradation of 3Y-TZP bulk ceramic in wet environment, many researches have been conducted on this phenomenon. Among the common features about low temperature degradation,[9–13] the grain size was regarded as one of the key factors to improve the resistance to the low temperature degradation in wet atmosphere. It had been found that zirconia bulk ceramic with a smaller grain size exhibited a better resistance to low temperature degradation.

In addition, plasma sprayed zirconia coatings have a metastable tetragonal-prime (t') crystal structure, and the t' phase shows high resistance to stress-induced transformation to the monoclinic phase.[14–19] If plasma sprayed zirconia coatings had the t' phase crystal structure and its grain size was less than the critical grain size of tetragonal phase, e.g., 0.3 μm for 3Y-TZP reported by Schmauder and Schubert,[20] the plasma sprayed zirconia coatings should have the best resistance to low temperature degradation. Our previous works demonstrated that nanostructured 3 mol% yttria stablized zirconia coatings can be deposited by plasma spraying technology,[21,22] and the nanostructured coatings had the metastable tetragonal-prime (t') crystal structure. Its average grain size was less than 100 nm. However, few reports on low temperature degradation of plasma sprayed nanostructured zirconia coatings can be found. So, the objective of this work is to investigate the low temperature degradation of plasma sprayed nanostructured zirconia coatings.

* Corresponding author. Tel.: +86 335 8074728; fax: +86 335 8501191.
E-mail address: liangbo1205@126.com (B. Liang).

0955-2219/$ – see front matter © 2009 Elsevier Ltd. All rights reserved.
doi:10.1016/j.jeurceramsoc.2009.01.002

Table 1
Plasma spray parameters.

Parameters	
Ar_2 (slpm)	35
H_2 (slpm)	12
Spraying distance (mm)	120
Gun current (A)	620
Power (kW)	42
Carrier air (slpm)	3.5

In the present work, nanostructured 3 mol% yttria stablized zirconia coatings were deposited by atmospheric plasma spraying. The structural evolutions of as-sprayed coatings during low temperature ageing in wet atmosphere were examined by Raman spectroscopy. In addition, the corresponding wavelength dispersive spectrometer (WDS) analysis was also carried out.

2. Samples and experimental procedures

Commercial nano-sized zirconia powders (3 mol% Y_2O_3) with grain sizes ranging from 30 to 80 nm (Fanmeiya Corp., Jiujiang, China) were used as the starting particles and reconstituted into micrometer-sized granules by spray drying process.

Three nanostructured coatings with a thickness of about 2×10^{-3} m were deposited on an aluminium alloy substrate using a Metco A-2000 atmospheric plasma spraying equipment (Sulzer Metco AG F4 gun, Switzerland). A mixture of argon and hydrogen was used as the plasma forming gas. Compressed air was used as cooling gas during plasma spraying. The optimum plasma spray parameters were listed in Table 1. After spraying, the as-sprayed coating was removed from the aluminium alloy substrate, then cut into 10 mm × 10 mm × 2 mm specimen using a SYJ-150A low speed diamond wheel saw cutoff machine (MTI Corporation, USA).

Two different ageing experiments were designed to investigate the low temperature ageing. One was carried out in the water bath (CU600, Zhisun, Shanghai) at 40, 60, 80 °C for 120 h and 100 °C for 24 h. The other was in water vapor at the 0.133 Pa pressure of water vapor. In the latter, the specimens were firstly put into an evacuated sealed silica tube, which was positioned in the tubular furnace, then aged in a steam of humid air with a flow rate of 10 mL/min at 250, 450, 650 °C for 30 h. The schematic illustration of the water vapor experiment apparatus was shown in Fig. 1.

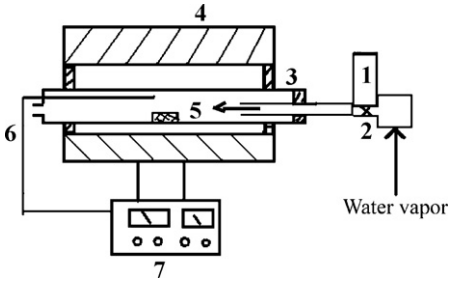

Fig. 1. Schematic diagram of experimental apparatus. 1: water vapor flowmeter; 2: needle valve; 3: quartz tube; 4: furnace; 5: specimen; 6: thermocouple; 7: temperature controller.

The phase evolution of aged coatings was identified by a LabRam-1B micro-Raman spectrometer (Dilor, France). For Raman spectrum analysis, the radiation of the 632.8 cm^{-1} line from a He–Ne laser was used as the excitation source and with 6.4 mW incident power and 100 s for each specimen. The main reason for using Raman spectroscopy in this study is that the tetragonal and monoclinic polymorphs of zirconia are reported to have distinct and characteristic Raman spectra.[23–25] A small amount of tetragonal or monoclinic phase could be detected in a polycrystalline zirconia material by its distinguishing lines. The monoclinic doublet (at 181 and 192 cm^{-1}) and the tetragonal bands (around 148 and 264 cm^{-1}) are well separated over the range 100–1000 cm^{-1}.

The relative fraction of the monoclinic phase, f_m, was calculated based on the Raman intensities of monoclinic doublet (at 181 and 192 cm^{-1}) and the tetragonal bands (at 148 and 264 cm^{-1}) using the relation

$$f_m = \frac{I_m^{181} + I_m^{192}}{k(I_t^{148} + I_t^{264}) + I_m^{181} + I_m^{192}}$$

where the value of k was taken to be 0.97.[26,27] The superscripts refer to the Raman shift of the characteristic peaks; the subscripts, t and m, refer to the tetragonal and monoclinic phase, respectively.

The surface morphology and cross-section area of the nanostructured zirconia coatings were examined by field emission scanning electron microscope (FESEM, JSM-6700F, JEOL, Japan) and scanning electronic microscopy (SEM, EPMA-8705QH, Shimadzu, Japan). The concentration of yttrium in specimens after ageing in water at 100 °C for 24 h was determined by wavelength dispersive spectrometer (WDS, JXA-8100, JEOL, Japan).

3. Results and discussion

3.1. Characterization of nanostructured zirconia coatings

Fig. 2 presents the Raman spectra of the as-sprayed nanostructured zirconia coating. It can be seen that four Raman lines occurred at 153.7, 261.1, 472.8 and 642.8 cm^{-1} could be

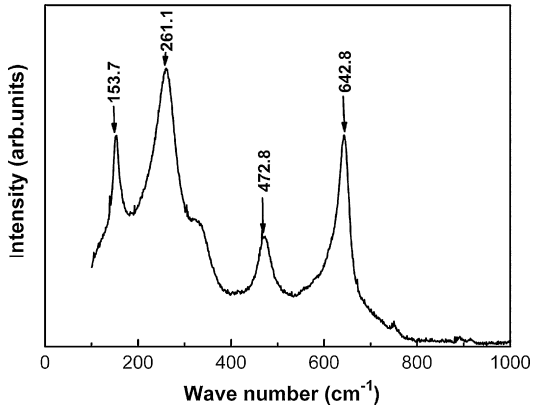

Fig. 2. The Raman spectrum of nanostructured 3 mol% yttria stabilized zirconia coatings.

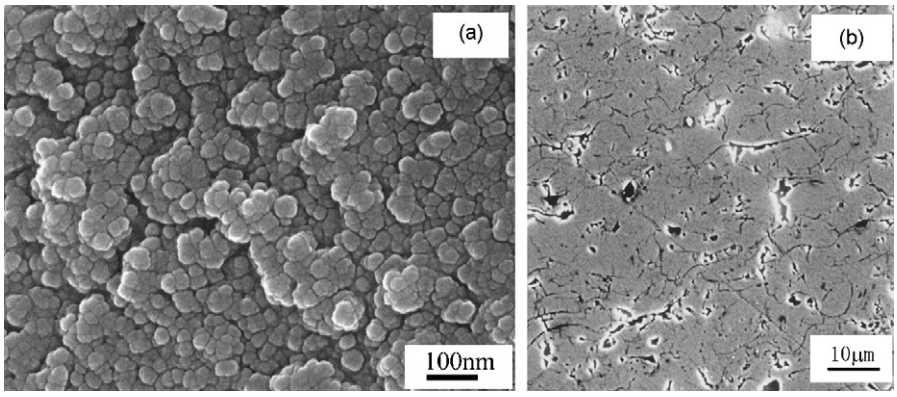

Fig. 3. (a) FESEM micrograph and (b) SEM micrograph of the cross-section of 3 mol% yttria stabilized zirconia coatings.

observed, they were identified with the typical characteristics of t' phase in our previous work.[21] No Raman lines of monoclinic and cubic phase were observed in Fig. 2. These results suggested that the primary crystal phase of the nanostructured zirconia coatings was t' phase. Comparing the obtained Raman lines of t' phase with the characteristic Raman lines of tetragonal zirconia phase reported in the literatures,[25–27] it can be found that the Raman lines of t' phase demonstrated some discrepancies in Raman numbers, e.g., a shift of $\approx 6\,cm^{-1}$ at $148\,cm^{-1}$, and $3\,cm^{-1}$ at $264\,cm^{-1}$. The observed shifts could be mainly assigned to the structural disorder and lower symmetry of the metastable tetragonal-prime (t') crystal phase. The lattice constants of tetragonal-prime (t') crystal phase were obviously lower than that of tetragonai phase, and the typical superlattice phenomenon was detected by TEM analysis.[21] It was caused by the distortion of the atomic array. The structural disorder of t' phase was formed due to the high quenching rate during plasma spraying process. In addition, the partial substitution of Zr with Y also resulted in the decrease of symmetry of t' phase.

Fig. 3(a) presents the FESEM micrograph of the nanostructured zirconia coatings. It clearly shows that the surface grains of the as-sprayed coatings are less than 100 nm in size. Fig. 3(b)

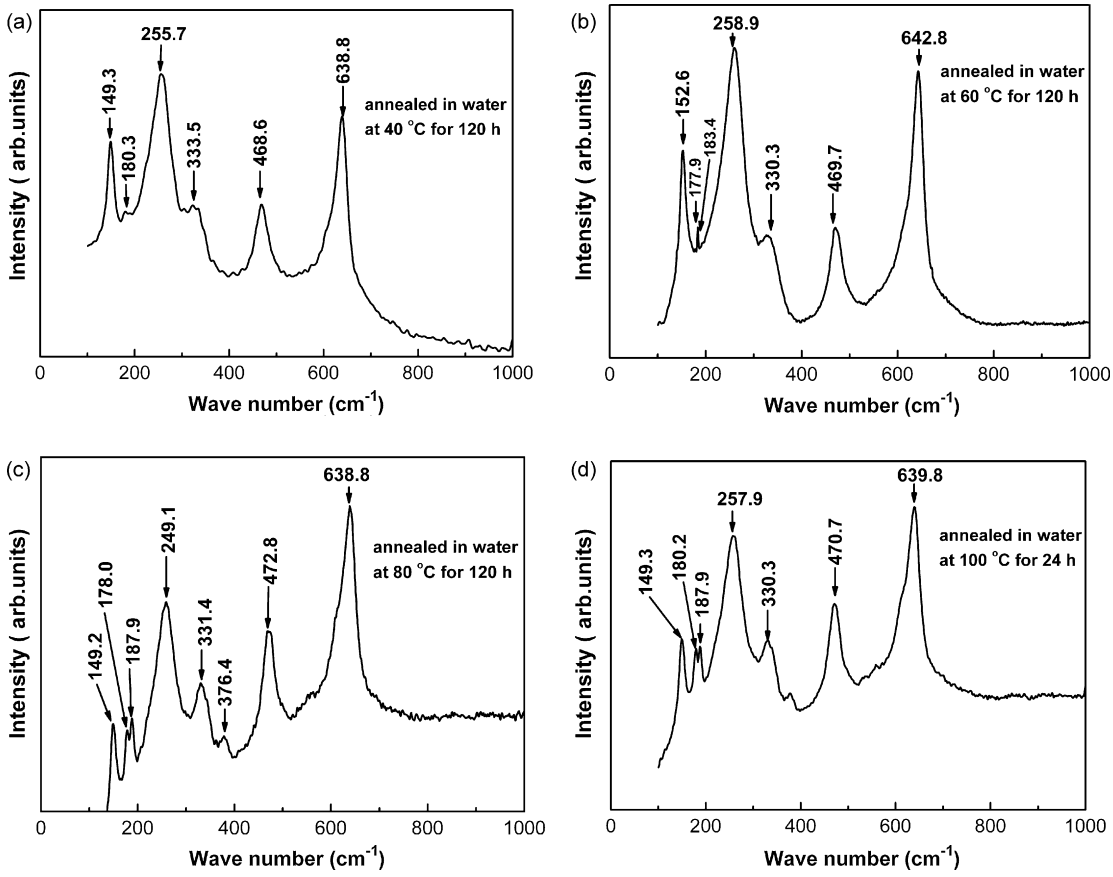

Fig. 4. The Raman spectra of the samples aged in water at different ageing temperature and time (a) 40 °C, 120 h; (b) 60 °C, 120 h; (c) 80 °C, 120 h and (d) 100 °C, 24 h, respectively.

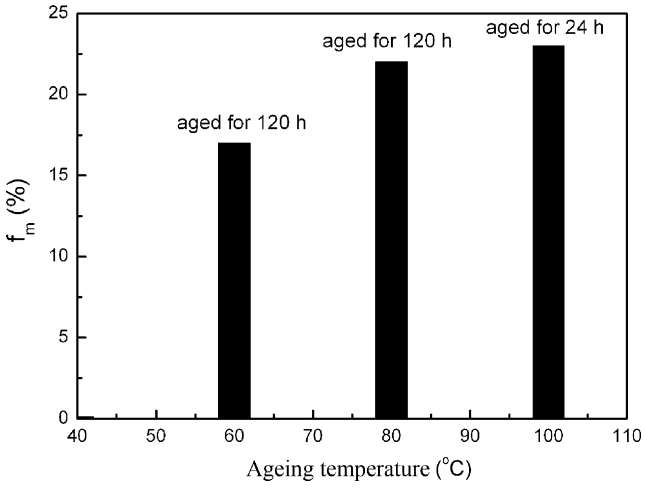

Fig. 5. The relative fraction of monoclinc phase (f_m) versus ageing temperature.

presented the SEM micrograph of the cross-section of the nanostructured zirconia coatings. From Fig. 3(b), it can be seen that there exists many microcracks and fine pores. The average diameter size of pores was less than 10 μm. The open porosity of as-sprayed nanostructured coatings is about 9% calculated using Archimedes method, the density was about 4.89 g/cm^3. The higher open porosity and the more microcracks are beneficial to the immersion of water.

3.2. Ageing in water

Fig. 4 presented the Raman spectra of nanostructured zirconia coatings aged in water at temperature 40, 60, 80 °C for 120 h and 100 °C for 24 h. From Fig. 4(a), it can be seen that no characteristic doublet lines occurring at 180 and 190 cm^{-1} of monoclinic phase were observed, when specimen was aged at 40 °C for 120 h in water. However, the characteristics doublet lines of monoclinic phase were obviously observed in the spectra of coatings aged at 60, 80 °C for 120 h in water (Fig. 4(b) and (c)), and at 100 °C for 24 h (Fig. 4(d)).

The relative fraction of monoclinic phase, f_m, was shown in Fig. 5. It can be seen from Fig. 5 that the f_m values increased from zero to 23% when ageing temperature increased from 40 to 100 °C. This result indicates that the transformation of t' to monoclinic phase was closely related to ageing temperature and time in water.

Fig. 6(a) presented the Raman spectra of coatings aged in water at 100 °C for 24 h recorded at 5, 15, 25 μm distance from surface to inner in depth. The corresponding f_m values calculated were 22%, 18% and 16% (shown in Fig. 6(b)). From Fig. 6(b), it can be concluded that with the increase of distance from surface to inner, the relative fraction of monoclinic phase decreased. This indicates that the transformation of t' to monoclinic phase mainly occurred in the surface of coatings when specimen was aged in water.

3.3. Ageing in water vapor

Fig. 7(a)–(c) presented the Raman spectra of nanostructured coatings aged in water vapor atmosphere at 250, 450 and 650 °C for 30 h. The corresponding f_m values were presented in Fig. 7(d). When comparing Fig. 7(a) with Fig. 7(b) and (c), it can be found that the intensities of the characteristic doublet lines of monoclinic phase were gradually reduced with the increase of ageing temperature, and it disappeared when ageing at 650 °C for 30 h. The corresponding f_m values calculated were 16%, 4% and 0, respectively (shown in Fig. 7(d)). These results showed that the transformation of t' phase to monoclinc phase did not occur in water vapor atmosphere when the ageing temperature was more than 650 °C.

3.4. Discussion

Although the nanostructured 3 mol% yttria stabilized zirconia coating had the metastable tetragonal-prime (t') crystal structure and its average grain size was less than 100 nm, the low temperature degradation was still observed in wet atmosphere and its ageing behavior was similiar as that of 3 mol% yttria stabilized zirconia bulk ceramic materials reported in many literaures.[9–14] We think, the ageing behaviors of nanostructured 3 mol% yttria stabilized zirconia coating can be explained using a degradation mechanism based on defect reaction. This degradation mechanism was proposed by Guo.[30,31] According to this

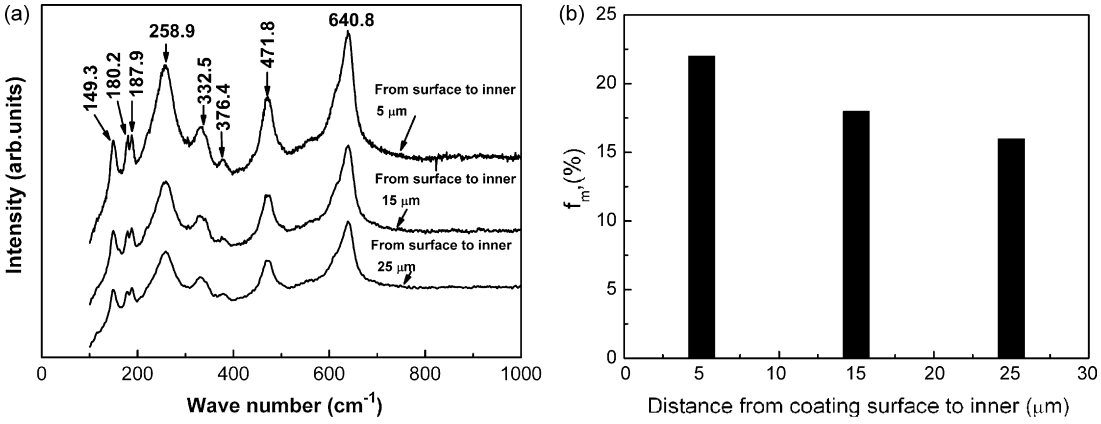

Fig. 6. The Raman spectra of the samples aged at 100 °C for 24 h in water (a) Raman spectra obtained at 5, 15 and 25 μm depths from the surface to inner and (b) the corresponding f_m values.

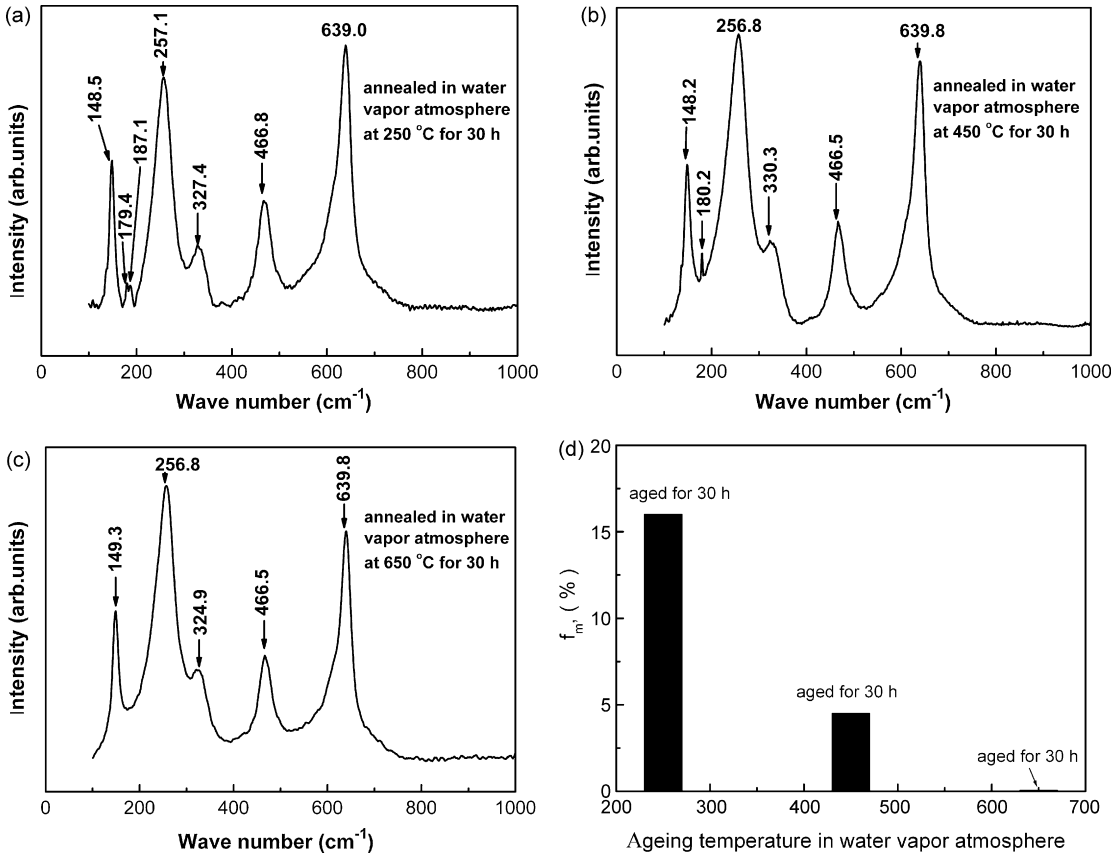

Fig. 7. The Raman spectra of the samples aged in water vapor atmosphere at (a) 250 °C, 30 h; (b) 450 °C, 30 h; (c) 650 °C, 30 h; (d) the corresponding f_m values.

degradation mechanism, oxygen vacancies play a very important role in the degradation, and the degradation probably results from some kinds of process involving oxygen vacancies. Oxygen vacancies can be annihilated by the incorporation of water molecules based on the following defect reaction:

$$H_2O + V_o^{\cdot\cdot} + O_o^x \Leftrightarrow 2(OH)_o^{\cdot} \quad (1)$$

So, the main degradation process can be described: (1) chemical adsorption of H_2O on zirconia surface, and reaction with O^{2-} to form hydroxyl groups OH^-; (2) OH^- penetration into the inner part by grain boundary diffusion, and annihilation of oxygen vacancies by OH^-; (3) when the oxygen vacancy concentration is reduced, the tetragonal phase is no longer stable, the tetragonal to monoclinic transformation occur. If the amount of the phase transformation is large enough, cracks can be produced, and cracks open up new surfaces to react with water molecules, leading to a further spontaneous transformation.

For plasma sprayed nanostructured 3 mol% yttria stabilized zirconia coating, the destabilization of t' phase also resulted from the diffusion of oxygen and OH^- ions when coating was aged in wet atmosphere.[7,28–31] The first step of degradation was the chemical adsorption of H_2O at the coating surface. Then, the adsorbed water could dissociate to form OH^- ions on the surface of as-sprayed coatings. This reaction between the H_2O molecule and oxygen on the coating surface can be described using Kröger–Vink notation as follows[30]:

$$H_2O_{ad} + O''_{surf} \rightarrow 2(OH)'_{surf} \quad (2)$$

where H_2O_{ad} is an adsorbed water molecule; O''_{surf} is oxygen on the surface; OH'_{surf} is an OH^- ion on the coating surface.

After the reaction, $V_{\ddot{o}}$ and/or $(OH)'_{surf}$ diffuse from coating surface to inner, a further defect reaction may occur as

$$(OH)'_{surf} + V_o^{\cdot\cdot} \rightarrow (OH)_o^{\cdot} + S^{\times}_{o.surf} \quad (3)$$

where $(OH)_o^{\cdot}$ is an OH^- ion on the oxygen site in the lattice; $S^{\times}_{o,surf}$ is a vacant surface site for oxygen. $V_{\ddot{o}}$ is the oxygen vacancy which is created to achieve electrical neutrality in the distorted fluorite lattice as Y^{3+} substitutes for Zr^{4+}. At last, some OH^- ions were introduced into lattice of t' phase and some oxygen vacancies were annihilated. Because the oxygen vacancy is the charge carrier, its diffusion to some extent is very diffcult at the ageing temperature. But the OH^- ions would be much faster than the oxygen vacancies due to the similar size as oxygen vacancies and less charge. As a result, in the nanostructured 3 mol% yttria stabilized zirconia coatings, the major diffusion species during ageing is OH^- ions.

In addition, the grain boundaries which is the main path for diffusion of OH^- ions also play an important role in ageing. The reaction between the OH^- ions and oxygen vacancies on the t' phase grain boundaries should not be neglected. This reaction

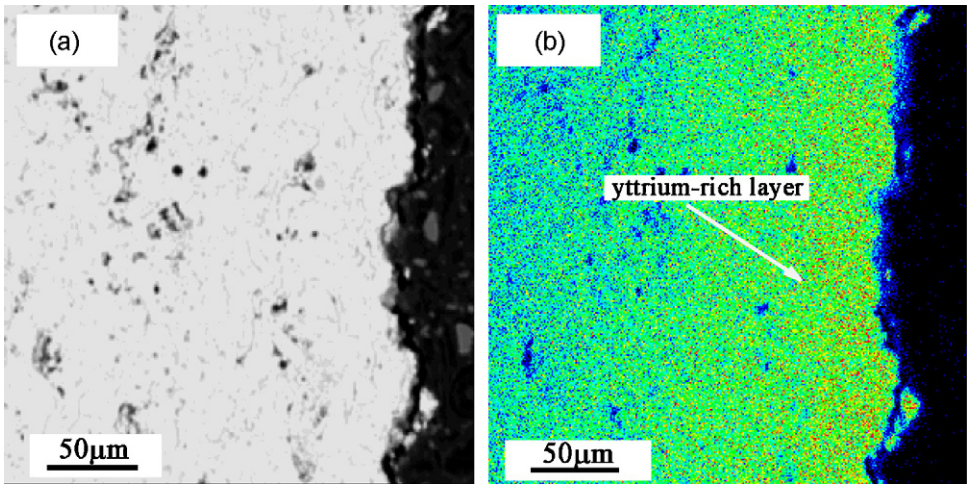

Fig. 8. WDS analysis of the samples aged at 100 °C for 24 h in water: (a) The SEM micrograph of cross-section of the samples and (b) the area scanning result of yttrium element.

can be written as[30,31]

$$(OH)'_{gb} + V_o^{\cdot\cdot} \rightarrow (OH)_o^{\cdot} + S_{o,gb}^{\times} \quad (4)$$

where $(OH)'_{gb}$ is an OH^- ion on the t' phase grain boundaries, $S_{o,gb}^{\times}$ is a vacant t' phase grain boundary site for oxygen. It has been verified that YSZ grain boundaries have a similar defect structure on the surface, thus, the t' phase grain boundary is also vulnerable to OH^- ion attack, just like what occurred on the surface of as-sprayed coatings, and the oxygen vacancies were also annihilated. It is well known that there are a critical minimum and maximum oxygen vacancy concentration for the stabilization of zirconia,[32] and the oxygen vacancy concentration variation should result in the phase transformation.

In the present work, it can be seen that by reaction Eqs. (3) and (4), the oxygen vacancy concentration not only on the surface but also on the grain boundaries of t' phase grains is reduced due to the annihilation by OH^-. When the oxygen vacancy concentration is reduced to such a critical extent that the t' phase destabilization may occur. On the other hand, the continuous diffusion of oxygen vacancies and/or OH^- ions can result in an accumulation residual stress and distort the Zr–O bonds on the surface.[33] This also facilitates the t' phase to monoclinic transformation during ageing.

Secondly, the microstructure of plasma sprayed nanostructured zirconia coating would enhance and accelerate the degradation of coatings. Because the microcracks can act as the preferential paths for water diffusion inside the inner of the coatings, thus accelerating the degradation of as-sprayed coatings. In our previous work,[21] it has been verified that more microcracks whose length is less than 10 μm were observed in the nanostructured 3 mol% yttria stabilized zirconia coatings. Although decreasing the grain size can increase the diffusion path of OH^- ions, which may retard the degradation. This effect may be neglected, if compared with that of microcracks on degradation. So, the effect of small grain size on degradation is less remarkable in the present work.

An yttrium-rich layer was observed on the surface of aged nanostructured coatings using WDS analysis technique. Fig. 8 presents the WDS analysis result of as-sprayed coatings aged at 100 °C for 24 h in water. It can be seen from Fig. 8(b) that the maximum yttrium concentration was observed on the coating surface, and the yttrium concentration was gradually decreased from surface to inner. This also can be explained by the coulombic interaction between charged defects and the Y'_{Zr} in the surface of coatings. This reaction may be schematically written as follows:

$$(OH)_o^{\cdot} + Y'_{Zr} \rightarrow Y(OH)_3 \quad (5)$$

where $(OH)_o^{\cdot}$ is an OH^- ion on the oxygen site in the lattice; Y'_{Zr} is an Y^{3+} ion on the zirconium site in the lattice. By the reaction Eq. (5), the $Y(OH)_3$ is formed. With the continuous reaction, an yttrium-rich surface layer was formed on the surface of nanostructured 3 mol% yttria stabilized zirconia coatings.

Although the degradation mechanism is still in dispute, the low temperature degradation may severely limit the application of plasma sprayed nanostructured zirconia coatings. Further works on the degradation mechanism of nanostructured zirconia coatings should be carried out.

4. Conclusions

(1) As far as the nanostructured 3 mol% yttria stabilized zirconia coatings deposited by plasma spraying are concerned, their resistance to low temperature degradation was lower. Their degradation mechanism can be contributed to the diffusion of oxygen vacancies and OH^- ion, which results in a reduction of oxygen vacancies concentration and the Zr–O band distortion. This facilitates the destabilization of t' phase grain during ageing.

(2) The microcracks observed in plasma sprayed nanostructured 3 mol% yttria stabilized zirconia coatings can enhance and accelerate the low temperature degradation when aged in wet atmosphere.

(3) An yttrium-rich surface layer could be formed on the surface of the aged coatings due to the reaction between $(OH)'_o$ and Y'_{Zr}, which may result in the transformation of t' to monoclinic zirconia.

Acknowledgements

This work was supported by Chine-France PRA dans le domaine des matériaux 2002 under PRA grant MX02-03 (C. Coddet & C. Ding).

References

1. Padture, N. P., Gell, M. and Jordan, E. H., Thermal barrier coatings for gas–turbine engine applications. *Science*, 2002, **296**, 80–84.
2. Hjelm, L. N. and Bornhorst, B. R., Development of improved ceramic coatings to increase the life of XLR 99 thrust chamber. Research Airplane-Committee Rept. on Conf. on Progress of the X-15 Project. *NASA TM* X-57-72, 1961. pp. 227–53.
3. Clarke, D. R. and Levi, C. G., Materials design for the next generation thermal barrier coatings. *Annu. Rev. Mater. Res.*, 2003, **33**, 383–417.
4. Taylor, R., Brandon, J. R. and Morrell, P., Microstructure, composition and property relationships of plasma sprayed thermal barrier coatings. *Surf. Coat. Technol.*, 1992, **50**, 141–149.
5. Miller, R. A., Smialek, J. L. and Garlick, R. G., Phase stability in plasma sprayed partially stabilized zirconia–yttria. In *Advances in Ceramics, Science and Technology of Zirconia, vol. 3*, ed. A. H. Heuer and L. W. Hobbs. The American Ceramic Society, Columbus, OH, 1981, pp. 241–253.
6. Brandon, J. R. and Taylor, R., Phase stability of zirconia-based thermal barrier coatings. Part I. Zirconia yttria alloys. *Surf. Coat. Technol.*, 1991, **46**, 75–90.
7. Wirgen, J. and Pejryd, L., Thermal barrier coatings—why, how, where and where to. In *Proceedings of the 15th international thermal spray conference*, 1998, pp. 1531–1542.
8. Parks, W. P., Hoffman, E. E., Lee, W. Y. and Wright, I. G., Thermal barrier coatings issues in advanced land-based gas turbines. *J. Thermal. Spray. Technol.*, 1997, **6**(2), 187–192.
9. Kobayashi, K., Kuwajima, H. and Masaki, T., Phase change and mechanical properties of ZrO_2–Y_2O_3 solid electrolyte after ageing. *Solid State Ionics*, 1981, **3/4**, 489–493.
10. Krajewski, A., Ravaglioli, A., Meschke, F., Azzoni, C. B., Crosignani, E., Scardina, F. *et al.*, Transformations on the surface of steam treated TSZ ceramics. In *Third Euro-Ceramics, Engineering Ceramics, vol. 3*, ed. P. Duran and J. F. Fernandez. Faenza Editrice Iberica S.L., 1993, pp. 518–528.
11. Sato, T. and Shimada, M., Crystalline phase changes in yttria-partially-stabilized zirconia by low-temperature annealing. *J. Am. Ceram. Soc.*, 1984, **67**(10), c212–c213.
12. Sato, T. and Shimada, M., Transformation of yttira-doped tetragonal ZrO_2 polycrystals by annealing in water. *J. Am. Ceram. Soc.*, 1985, **68**(6), 356–359.
13. Lawson, S., Environmental degradation of zirconia ceramics. *J. Eur. Ceram. Soc.*, 1995, **15**, 485–502.
14. Yoshimura, M., Noma, T., Kawabata, K. and Somiya, S., Role of H_2O on the degradation process of Y-TZP. *J. Mater. Sci. Lett.*, 1987, **6**, 465–467.
15. Ingel, R. P., Lewis, D., Bender, B. A. and Rice, R. W., Temperature dependence of strength and fracture toughness of ZrO_2 single crystals. *J. Am. Ceram. Soc.*, 1982, **65**(9), C150–C152.
16. Heuer, A. H., Chaim, R. and Lanteri, V., The displacive cubic to tetragonal transformation in ZrO_2 alloys. *Acta Metall.*, 1987, **35**(3), 661–666.
17. Sakuma, T., Yoshizawa, Y. and Suto, H., The microstructure and mechanical properties of yttria stabilized zirconia prepared by arc melting. *J. Mater. Sci.*, 1985, **20**, 2399–2407.
18. Jue, J. F., Chen, J. and Virkar, A. V., Low temperature aging of t' phase zirconia: the role of microstructure on phase stability. *J. Am. Ceram. Soc.*, 1991, **74**(8), 1811–1820.
19. Michel, D., Mazerolles, L. and Jorba, M. P., Fracture of metastable tetragonal zirconia crystals. *J. Mater. Sci.*, 1983, **18**, 2618–2628.
20. Schmauder, S. and Schubert, H., Significance of internal stresses for the martensitic transformation in yttria stabilized tetragonal zirconia polycrystals during degradation. *J. Am. Ceram. Soc.*, 1986, **69**(7), 534–540.
21. Liang, B. and Ding, C. X., Phase composition of nanostructured zirconia coatings deposited by air plasma spraying. *Surf. Coat. Technol.*, 2005, **191**, 267–273.
22. Chen, H., Zeng, Y. and Ding, C. X., Microstructural characterization of plasma sprayed zirconia powders and coating. *J. Eur. Ceram. Soc.*, 2003, **23**(3), 491–497.
23. Ghosh, A., Suri, A. K. and Pandey, M., Nanocrystalline zirconia yttria system—a Raman study. *Mater. Lett.*, 2006, **60**, 1170–1173.
24. Baklanova, N. L., Kolesov, B. A. and Zima, T. M., Raman study of yttria stablized zirconia interfacial coatings on Nicalon™ fiber. *J. Eur. Ceram. Soc.*, 2007, **27**, 165–171.
25. Moura, C., Carvalho, P., Vaz, F., Cunha, L. and Alves, E., Raman spectra and structural analysis in ZrO_xN_y thin film. *Thin Solid Films*, 2006, **515**, 1132–1137.
26. Phillippi, C. M. and Mazdiyasni, K. S., Infrared and Raman spectra of zirconia polymorphs. *J. Am. Ceram. Soc.*, 1971, **54**(5), 254–258.
27. Keramidas, V. G. and White, W. B., Raman scattering study of the crystallization and phase transformations of ZrO_2. *J. Am. Ceram. Soc.*, 1974, **57**(1), 22–24.
28. Lange, F. F., Dunlop, G. L. and Davis, B. I., Degradation during ageing of transformation toughened ZrO_2–Y_2O_3 materials at 250 °C. *J. Am. Ceram. Soc.*, 1986, **69**, 237–240.
29. Hernandez, M. T., Jurado, J. R. and Duran, P., Subeutectoid degradation of yttria stabilized tetragonal zirconia polycrystal and ceria doped yttria stabilized tetragonal zirconia polycrystal ceramics. *J. Am. Ceram. Soc.*, 1991, **74**(6), 1254–1258.
30. Guo, X., On the degradation of zirconia ceramics during low temperature annealing in water or water vapor. *J. Phys. Chem. Solids*, 1999, **60**, 539–546.
31. Guo, X., Property degradation of tetragonal zirconia induced by low-temperature defect reaction with water molecules. *Chem. Mater.*, 2004, **16**(21), 3988–3994.
32. Badwal, B. P. S. and Nardella, N., Formation of monoclinic zirconia at the anodic face of tetragonal zirconia polycrystalline solid electrolytes. *Appl. Phys. A*, 1989, **49**, 13–24.
33. Kim, D.-J., Influence of aging environment on low temperature degradation of tetragonal zirconia alloys. *J. Eur. Ceram. Soc.*, 1997, **17**, 897–903.